

## Analysis on passenger flow evolution and service facility configuration for large-scale events in outer suburbs

Huanmei Qin<sup>1</sup>, Meiru Jia<sup>2</sup>, Cui Qian<sup>3</sup>, Yonghuan Zhang<sup>4</sup>

<sup>1</sup> corresponding author [hmqin@bjut.edu.cn](mailto:hmqin@bjut.edu.cn), Beijing Key Lab of Traffic Engineering, Beijing University of Technology, Beijing 100124, China;

<sup>2</sup> Shijiazhuang Institute of Technology, Shijiazhuang 050228, China;

<sup>3</sup> Beijing Key Lab of Traffic Engineering, Beijing University of Technology, Beijing 100124, China;

<sup>4</sup> Beijing Key Lab of Traffic Engineering, Beijing University of Technology, Beijing 100124, China;

### Keywords

*Large-scale events in outer suburbs*  
*Passenger flow evolution*  
*Service facility configuration*  
*Queuing time*

### Publishing history

Submitted: 5 September 2023

Revised date(s): 9 July 2024

Accepted: 26 July 2024

Published: 19 September 2024

### Cite as

Qin, H., Jia, M., Qian, C., & Zhang, Y. (2024). Analysis on passenger flow evolution and service facility configuration for large-scale events in outer suburbs. *European Journal of Transport and Infrastructure Research*, 24(3), 17-40.

©2024 Huanmei Qin, Meiru Jia, Cui Qian, Yonghuan Zhang.

This work is licensed under a Creative Commons Attribution 4.0 International License (CC BY 4.0)

### Abstract

As more and more large-scale winter events are held in different areas, a reasonable configuration of service facilities is crucial for ensuring the successful execution of these events. Based on an analysis of the passenger flow for large-scale events in outer suburbs, this study has developed a dynamic evolution model to well simulate passenger arrival distribution among nodes and queue performance over time. Subsequently, an optimization model for service facility configuration based on node linkage is proposed. Using a large-scale winter event as a case study, we conclude that assigning a higher objective weight to spectators' queuing time cost in the optimization model leads to an increase in the number of configured service facilities among nodes, thereby enhancing service quality. Different facility layouts for security checks and ticket checks have no significant effects on the optimal number of configured service facilities and spectator queuing time costs. However, implementing a remote security check can alleviate passenger congestion at downstream nodes and reduce the overall queuing time cost. The dynamic evolution model and the service facilities configuration model are suitable for coordinating passenger flow under limited-service facility provision along with measures such as adjusting facility layouts and controlling passenger flow. Thus, a good match between passenger flow distribution and facility service capacity can be achieved. The research conclusions can provide a reference for the analysis of passenger flow, service facility configuration, and passenger flow organization for large-scale events held in the outer suburbs.

## 1 Introduction

With the rapid development of the economy, an increasing number of large-scale events are taking place in various areas. Meanwhile, the patterns of the events have become more novel, leading to diverse demands, particularly for large-scale winter events. Typically, some urban venues are unable to meet the requirements of winter events. Consequently, it is necessary to construct venues in remote mountainous regions surrounding the city, where colder climates and abundant ice and snow are present.

The large-scale winter events hosted in the outer suburbs share many characteristics with ordinary large-scale events, capable of attracting large crowds within a short period of time and assembling people in a limited space. However, these suburban events also have unique features of lower traffic accessibility, more transfer points, complex traffic conditions, etc. For instance, spectators traveling from downtown to the venue may encounter multiple service facilities including transfer station, security check, ticket check, and diversion areas, all of which bring great challenges to passenger flow organization. Inadequate service facility configuration can lead to assembling passenger flow along the travel route and a decline in service level. Coupled with cold weather, spectators' travel experiences are seriously affected, and safety incidents may even occur. Conversely, an excessive allocation of service facilities If the service facilities are redundantly configured would be a wasteful use of resources, driving up operational costs. Thus, a reasonable configuration of service facilities is crucial to ensure the successful holding of the large-scale winter events.

Based on an analysis of the passenger flow entry process from downtown to the venue, this study established a dynamic evolution model of passenger flow and proposed an optimization method for service facility configuration with node linkage tailored for large-scale events. Using a winter event held in the outer suburb as a case study, the influence of the objective weight of the facility configuration and changes in facility layout on passenger flow distribution, and service quality was discussed. Additionally, the study explores the organization and optimization methods of passenger flow within the capacity constraints of service facilities. The research conclusions can provide a reference for passenger flow analysis, service facility configuration, and passenger flow organization for large-scale events held in outer suburbs.

## 2 Literature review

Currently, many large-scale events have been held in various cities, and there is a summary of experiences in passenger flow organization and facility optimization. Roper (1987) proposed traffic organization and management methods to improve day-to-day travel patterns for the 1984 Los Angeles Olympic Games, based on an analysis of traffic conditions. Similarly, Frantzeskakis (2006) studied the planning and management of transportation infrastructure for the 2004 Athens Olympic Games, and used simulation models and prediction tools to estimate Olympic traffic movements. Karlaftis et al. (2006) introduced a decision support system (DSS) to support the planning and operation of a special shuttle bus network for large-scale events, taking into account the limited infrastructure and resources, as well as the uncertainties of the passenger flow arrival.

In terms of the characteristics of passenger flow for large-scale events (Fellendorf, 2006), Wei et al. (2009) conducted a study on the characteristics of pedestrian flow during the ingress and egress of the Sudirman Semi-final in Beijing and used LEGION software to enhance the service level. Zhang et al. (2015) took the 9th China International Garden Expo as their research object and analyzed the characteristics of passenger arrivals, delving into the influence of various factors such as climate, precipitation, featured activities, holidays, and others on passenger volume. Li et al. (2019) analyzed the spatiotemporal features of passenger flow at the Beijing International Auto Show and the 9th China International Garden Expo and explored the daily, weekly, and monthly changes in passenger flow.

Regarding the configuration and optimization of service facilities, Liu et al. (2018) established a queuing theory model aimed at addressing the safety problems arising from spectators' crowded queues for security checks of sporting events. The model was also used to optimize the layout of service facilities, thereby mitigating the risk of crowd aggregation. Matthew (2004) developed a decision support system and an auxiliary public transportation optimization model for the traffic organization of large-scale events. These methods were successfully applied to the operation scheme of public transport during the 2004 Olympic Games in Athens. To ensure efficient evacuation of passenger flow in large-scale events, Zhang (2003) formulated a mathematical optimization model and used public transport as the primary evacuation mode, capitalizing on its large capacity and centralization benefits. Some studies have also delved into the analysis of service facilities for security and ticket checks at airports. Considering passenger arrival and the configured facilities for security checks, Ding et al. (2018) established a queuing model grounded in queuing theory to analyze the impact of the number of security gates on reducing passenger waiting time. Yi (2016) analyzed passenger flow along airport security lines, establishing a queuing model specific to security checkpoints and proposing enhancements to alleviate long wait times. The aforementioned studies primarily employed queuing theory and mathematical models to optimize a certain type of service facility for an event. Few studies have focused on optimizing the facility configuration for large-scale winter events held in the outer suburbs, taking into account the evolving process of passenger flow across different facility nodes.

Regarding the collaborative optimization of passenger flow and service capacity of facilities, related research has predominantly concentrated on rail transit (Wang et al, 2019; Wang et al, 2022). Yoo et al. (2022) controlled inbound passenger flow by reducing the service capacity of the ticket-checking facilities, leading to a decreased queuing time for passengers on the platform. Yin et al. (2021) established a single-line equilibrium passenger flow control model aimed at minimizing the total delay. By controlling the service capacity of the security-checking facilities, the passenger flow can be evenly distributed among different platforms, thereby minimizing overall passenger flow delay. Wang et al. (2020) proposed an optimization method for passenger flow distribution that can control the inbound passenger flow by changing the passage efficiency of security-checking facilities. Combined with the passengers' arrival distribution on different platforms, it is proved that the method can minimize the total number of passengers waiting to board on the rail line. Liu et al. (2020) addressed the problem of large passenger flow for subway during the peak period. They proposed that the number of passengers waiting on the platform can be maintained at a moderate level by changing the passage efficiency of the service facilities, such as security-checking facilities. While these studies primarily focused on controlling passenger flow by changing facility service capacity to reduce waiting times, there is a notable scarcity of research on collaborative optimization of passenger flow and service facilities across multiple nodes for large-scale events.

In summary, while there are many studies on passenger flow analysis and facility configuration optimization at single station or service facility for rail transit and airports, limited research has been conducted specifically on large-scale winter events held in outer suburbs, taking into account their unique characteristics. These events are characterized by massive and strong passengers assembling, long route distances, more transfer points, and low traffic accessibility. Furthermore, travel behavior characteristics are also influenced by weather and traffic conditions prevalent in cold areas. Consequently, it is necessary to comprehensively consider the multi-node linkage operations and coordinated scheduling of transportation modes to optimize passenger flow organization during such events.

This research primarily explored the dynamic evolution of passenger flow among service facility nodes during the entry process from downtown to the venue, as well as the configuration optimization of service facilities. The main innovations are as follows. (1) A dynamic evolution model of the passenger flow is constructed for large-scale events. This model enables real-time passenger flow distribution at different facility nodes. (2) An optimization method based on the linkage of multiple facility nodes was proposed to explore the suitable number of service facility and the service quality under different facility layouts. (3) The optimization scheme of the

passenger organization under the capacity constraint of service facilities was devised to achieve a good match between the passenger flow distribution and facility service capacity.

### 3 Dynamic evolution model of passenger flow for large-scale events in outer suburbs

For large-scale events in the outer suburbs, passenger flow typically moves dynamically through various service facility nodes during their journey from downtown to the venue. The service facilities primarily refer to transport transfer facility, security-checking facilities, ticket-checking facilities, bus boarding and drop-off zone. The location of these service facility is defined as a facility node. The attractions, on the other hand, refer to shops, landscapes, and sculptures, which can entice people to stop and stay. They are often located between or adjacent to the facility nodes. The description of the research problem is illustrated in Figure 1.

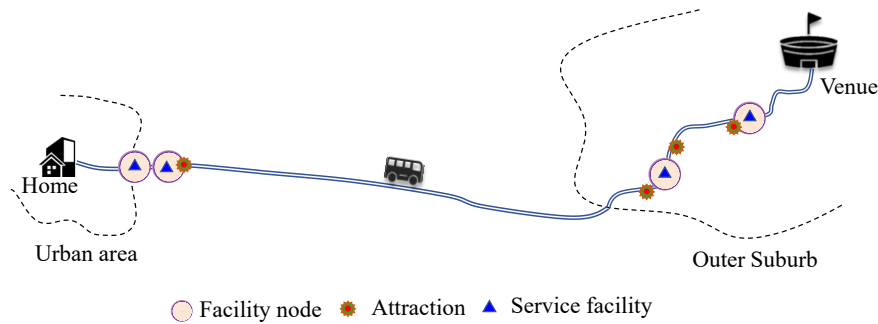


Figure 1. Schematic diagram of research problem

The passenger flow distribution and queuing time are influenced by the service capacity of the facilities at each node, and have a dynamic, correlated effect among the facility nodes from upstream to downstream. Consequently, it is necessary to develop an evolution model of passenger flow for large-scale events held in outer suburbs.

#### 3.1 Passenger arrival and inter-node travel time distribution

For the entry process of passenger flow from downtown to the venue, it is assumed that  $j$  represents the facility node and  $J$  represents the total number of nodes. Let  $k$  denote the type of attraction and  $K$  represents the total number of types. From the time when the first group of spectators arrives at the first facility node until all spectators reach the venue, the total time is denoted as  $T$ . The minimum time interval for the evolution model of passenger flow is set to one minute, and the passenger flow analysis is conducted at minute intervals for statistics.

The arrival distribution function of spectators at each facility node is assumed to be  $f_j(t)$ ,  $j = 1, 2, \dots, J$ , which represents the number of passengers arriving at facility node  $j$  at time  $t$ . The moment when the first group of spectators arrives at the first facility node is expressed as  $t = 0$ . The passenger arrival distribution at a facility node is influenced by the passenger departure distribution at its neighboring upstream node and the travel time between these two nodes.

The travel time between two adjacent facility nodes primarily consists of walking time, dwell time, and riding time by public transit, as detailed in Formula 1.

$$T_{j-1,j} = T_{j-1,j}^{walk} + T_{j-1,j}^{dwell} + T_{j-1,j}^{ridr} \quad (1)$$

where  $T_{j-1,j}$  is the time required for spectators to travel from node  $j-1$  to node  $j$ .  $T_{j-1,j}^{walk}$ ,  $T_{j-1,j}^{dwell}$ , and  $T_{j-1,j}^{ridr}$  are the walking time, dwell time, and riding time between two adjacent nodes, in minutes.

Considering spectators' individual differences in walking speed, it is assumed that walking time  $T_{j-1,j}^{walk}$  follows the distribution of  $f_{walk}(t)$ , as shown in Formula 2.

$$T_{j-1,j}^{walk} \sim f_{walk}(T_{j-1,j}^{walk}) = \frac{L_{j-1,j}}{\sqrt{2\pi\sigma(T_{j-1,j}^{walk})^2}} e^{-\frac{(L_{j-1,j}/T_{j-1,j}^{walk}-u)^2}{2\sigma^2}} \quad (2)$$

where  $L_{j-1,j}$  represents the distance between node  $j-1$  and node  $j$  in meters.  $u$  and  $\sigma^2$  are the mean and variance of the walking speed, respectively.

The dwell time between two adjacent facility nodes refers to the total time a passenger spends on staying at different types of attractions located between those two nodes. It is assumed that the dwell time follow a normal distribution, as shown in Formula 3.

$$T_{j-1,j}^{dwell} = \sum_{k=1}^K Z_{g_j(t)k} \times T_k^{dwell} \quad T_k^{dwell} \sim N(u_k, \sigma_k^2) \quad (3)$$

where  $T_{j-1,j}^{dwell}$  represents spectators' dwell time at  $K$  types of attractions.  $u_k$  and  $\sigma_k^2$  are the mean and variance of dwell time at the  $k$ -type attraction, respectively.  $Z_{g_j(t)k}$  is a 0-1 variable. If the spectators leaving from node  $j-1$  at time  $t$  to node  $j$  stay at the  $k$ -type attraction,  $Z_{g_j(t)k}$  is assigned to 1; otherwise, it is 0.

For the evolution model of passenger flow, spectators' walking and dwell times are randomly generated according to the aforementioned distribution functions.

The riding time is calculated using the distance between the two facility nodes and the average travel speed of the travel mode used by the spectator, as demonstrated in Formula 4.

$$T_{j-1,j}^{ridr} = \frac{L_{j-1,j}}{v} \quad (4)$$

where  $v$  is the average travel speed of the travel mode in metres per minute.

### 3.2 Dynamic evolution model of passenger flow at key facility nodes

During spectators' travel from downtown to the even in the outer suburbs, passenger arrival patterns vary at different facility nodes. Queues may well form due to the limited capacity of service facilities or pass efficiency. Therefore, spectators' queuing time at facility nodes is an important indicator for evaluating the reasonability of the service facilities configuration.

#### *Evolution model of passenger flow at security or ticket checkpoints*

Security checks and ticket checks are two essential services for large-scale events that can be modeled as one type of facilities due to their similar service characteristics. The real-time queuing time and passenger flow distribution at these nodes can be estimated by considering the relationship between passenger arrival and service capacity of the facilities.

- Service capacity for security checking or ticket checking facilities

The service capacity of a single security checking or ticket-checking gate can be calculated using Formula 5.

$$A_j = \frac{1}{D_j} \quad (5)$$

where  $A_j$  is the service capacity for a single security checking or ticket-checking gate in persons per minute.  $D_j$  is the average service time per person at node  $j$  in min.

If the number of configured service facilities at the node  $j$  is defined as  $N_j$ , the service capacity for a facility node  $j$  is calculated as  $A_j \times N_j$ .

The service intensity of the security checking or ticket-checking facilities can be expressed by Formula 6.

$$\rho_j(t) = \frac{f_j(t)}{q_j} \quad (6)$$

where,  $\rho_j(t)$  represents the service intensity of facility node  $j$  at time  $t$ .  $q_j$  is the service capacity for facility node  $j$  in persons per minute.

- Identification of the start and end times of the passenger queues

If the service intensity for a facility node  $j$  satisfies  $\rho_j(t) \leq 1$ , it is considered that the spectators arriving at node  $j$  at time  $t$  do not need to queue up. If  $\rho_j(t) > 1$ , queues are formed at node  $j$  at time  $t$ . It is assumed that the number of the queues formed at node  $j$  during the entire entry process is  $n_j$ . A single queue is defined as the entire process from its formation to dissipation. The start and end times of each queue are expressed as  $t_{Bx}^j$  and  $t_{Ex}^j$ , and  $x = 1, 2, \dots, n_j$ .

From the arrival of the first group of passenger flow at node  $j$ , the discriminant criteria are employed to identify whether a queue is formed at node  $j$  at time  $t$ .  $t_{B1}^j$  represents the start time of the first queue that appears at node  $j$ .  $t_{Bx}^j$  is the start time for the  $x$ th queue at node  $j$ , where  $x = 2, 3, \dots, n_j$  is expressed as the moment when the service intensity starts to be continuously greater than 1, as shown in Formula 7.

$$t_{Bx}^j = \left\{ \min t \mid \rho_j(t) > 1, t > t_{E(x-1)}^j \right\} \quad (7)$$

where,  $t_{E0}^j = 0$ .

The end time of the queue can be obtained by using Formula 8.  $t_{Ex}^j$  represents the moment when the accumulated passengers arriving in a queue start to be less than the service capacity of facility node  $j$ .

$$t_{Ex}^j = \left\{ \min t \mid F_j(t) - F_j(t_{Bx}^j) \leq \sum_{t_{Bx}^j}^t q_j(t) \right\} \quad (8)$$

- Real-time queuing time of spectators at security or ticket checkpoints.

When spectators' arrival is not within the identified queuing interval, their waiting time for security or ticket services is ignored. Otherwise, the average waiting time can be calculated by the mean value of the minimum and maximum queuing times for the spectators arriving at node  $j$  at time  $t$ , as shown in Formula 9.

$$T_j(t) = \begin{cases} 0, & t \in [1, t_{B1}^j] \cup [t_{E(n_j-1)}^j, t_{Bn_j}^j] \\ \frac{F_j(t) + F_j(t-1) - 2F_j(t_{By}^j - 1) - 2q_j \times (t-1 - t_{By}^j)}{2q_j}, & t \in (t_{B1}^j, t_{E1}^j) \cup (t_{Bn_j}^j, t_{En_j}^j) \end{cases} \quad (9)$$

where  $T_j(t)$  represents the spectators' average queuing time to be served at node  $j$  at time  $t$ .  $t_{By}^j$  represents the start time of the queuing interval, in which the arrival time  $t$  lies in  $t_{By}^j = (\max t_{Bx}^j \mid t \geq t_{Bx}^j)$ , where  $y = 1, 2, \dots, n_j$ .

- Passenger flow departing from security or ticket checkpoints

When spectators' arrival is not within the identified queuing interval, the passenger flow departing from the security or ticket checkpoint is consistent with their arrival distribution. When their arrival is within the queuing interval, the passenger flow departing from a node is equal to the service capacity of the facilities at the node. The passenger flow departing from node  $j$  at time  $t$  is expressed by Formula 10.

$$g_j(t) = \begin{cases} f_j(t), & t \in [1, t_{B1}^j] \cup (t_{E(n-1)_j}^j, t_{Bn_j}^j) \\ q_j, & t \in [t_{B1}^j, t_{E1}^j] \cup [t_{Bn_j}^j, t_{En_j}^j] \end{cases} \quad (10)$$

where  $g_j(t)$  represents the number of spectators departing from the node  $j$  at time  $t$ .  $f_j(t)$  represents the number of spectators arriving at node  $j$  at time  $t$  in persons per minute.

#### *Evolution model of passenger flow at public transport nodes*

It is assumed that spectators primarily use shuttle buses to travel from the urban transfer point to the venue in the outer suburbs for large-scale events. The operating mode of the shuttle bus is to depart once they are full. The direct shuttle buses are of uniform size and operate in a cyclic manner between the urban transfer point and the venue, with no intermediate stops. The time taken by spectators to board and disembark from the buses, as well as the time for buses to enter and exit the station, is neglected. The passenger arrival and average waiting time in the boarding area are modeled as follows:

- Number and time of departure for shuttle bus

It is assumed that  $C_b$  represents the capacity of a shuttle bus.  $N_j$  represents the total number of configured shuttle buses.  $T_{return}$  denotes the round-trip time of the shuttle bus.  $n_{need}(t)$  is the minimum number of vehicles required to transport passengers waiting at the pick-up point at time  $t$ , as shown in Formula 11. The existing passengers are calculated as the difference between the cumulative arrival of spectators at time  $t$  and the cumulative spectators transported by shuttle buses prior to time  $t$ .

$$n_{need}(t) = \left\lfloor \frac{F_j(t) - \sum_{x=0}^{t-1} s(x) \times C_b}{C_b} \right\rfloor \quad (11)$$

where  $s(x)$  is the number of departures for buses at time  $x$  and  $\lfloor x \rfloor$  represents rounding down the intermediate variable  $x$ .

The number of available vehicles at time  $t$  can be calculated using Formula 12. It equals the total number of configured shuttle buses  $N_j$  minus the departed vehicles and plus the returned

vehicles before time  $t$ . The number of returned vehicles equals those that left before the time of  $t - T_{return}$  and have since returned.

$$n_{exit}(t) = N_j - \sum_{x=0}^{t-1} s(x) + \sum_{x=0}^{t-T_{return}} s(x) \quad (12)$$

Therefore, the number of departures for buses at time  $t$  is the minimum value between the number of required vehicles and available vehicles at that time, as shown in Formula 13.

$$s(t) = \min \{n_{need}(t), n_{exit}(t)\} \quad (13)$$

Since many vehicles may need to be dispatched simultaneously, the departure time of the  $n$ th vehicle  $t_n^d$  is expressed as the minimum moment when the cumulative number of departures reaches  $n$ , as shown in Formula 14.

$$t_d^n = \min t \mid \sum_{x=0}^t s(x) \geq n \quad (14)$$

- Real-time queuing time of spectators at pick-up point

The  $F_j(t)$ th spectator who arrives at the pick-up point need to take the  $n(t)$ th shuttle bus to leave.

$$n(t) = \left\lceil \frac{F_j(t)}{C_b} \right\rceil \quad (15)$$

where,  $\lceil x \rceil$  means rounding up the intermediate variable  $x$ .

The departure time of the  $n(t)$ th shuttle bus is denoted by  $t_d^{n(t)}$ . Therefore, the average queuing time  $T_j(t)$  for spectators who arrive at the pick-up point  $j$  at time  $t$  is expressed as Formula 16.

$$T_j(t) = t_d^{n(t)} - t \quad (16)$$

- Passenger flow at the pick-up and drop-off points.

The passenger flow departing from the pick-up point is the product of the number of departed vehicles and the passenger capacity, as shown in Formula 17.

$$g_j(t) = s(t) \times C_b \quad (17)$$

where,  $g_j(t)$  represents the number of passengers departing from node  $j$  at time  $t$ .

Based on the passenger flow departing from the pick-up point, the arrival distribution at the drop-off point is obtained by displacing the riding time by the shuttle bus backward, as shown in Formula 18.

$$f_j(t) = s(t - T_{j-1,j}^{ridr}) \times C_b \quad (18)$$

where,  $j$  represents the drop-off point of shuttle bus.

### 3.3 Verification of dynamic evolution model for inbound passenger flow

To analyze the effectiveness of the dynamic evolution model for a large-scale winter event, video surveys and questionnaires were utilized to collect data on passenger flow and its behavioral characteristics

The Finlandia International Ski Marathon was held in Volga Manor in Harbin, China, from January 7 to 9, 2020. The temperature during the event ranges from approximately  $-20^\circ \text{C}$  to  $-15^\circ \text{C}$ . Figure



2 illustrates the manor's two entrances. Entrance 1 is adjacent to a car parking lot 1, while Entrance 2 is situated beside a visitor center, with a parking lot 2 approximately 50 meters away.

Spectators can take a group bus or drive a car to the parking lot and then walk through Routes 1 or 2 to reach the starting point of the competition. Route 1 is primarily catering to individual spectators, whereas Route 2 serves both group and individual spectators. Both routes are approximately 400 meters long. Some attractions, such as birch forests, sculptures, and shops, are distributed along the routes. There were six ticket-check machines at each entrance.

To monitor passenger flow, four cameras were placed at Entrance 1, Entrance 2, the intersection of Routes 1 and 2, and the starting point of the competition respectively along the entry routes. The survey was conducted on January 7, 2020, with a large number of spectators during the competition. The competition commenced at 10 o' clock. The behavioral characteristics of spectators were collected by the questionnaire, which includes dwell time at attractions and their acceptable queue waiting time for security checks, ticket checks, and public transport. A total of 625 valid samples were collected during the competition.



Figure 2. Entry routes and locations of cameras in the Manor

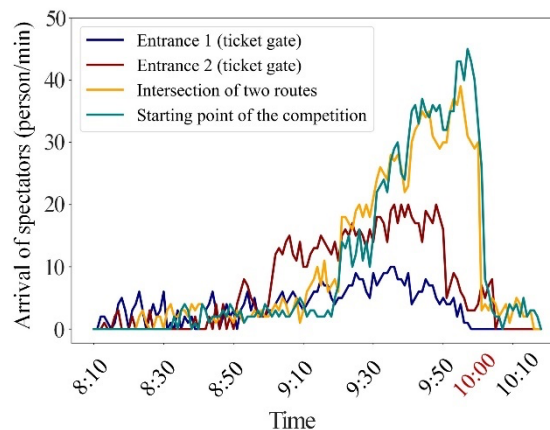


Figure 3. Arrival distribution of spectators at each node

Based on the video data, the passenger flow distribution at each node during the entry process is illustrated in Figure 3. It is evident that spectators began arriving at the manor's entrances one after another from 8:10 onwards and most of them are opt to proceed to the competition's starting point via Entrance 2 and Route 2. In general, the arrival distribution of the passenger flow initially increased and then subsequently decreased over time. For passenger flow at the two entrances, a large number of spectators arrive between 9:00 and 9:50, preceding the competition's commencement. The peak flow at these two entrances appears between 9:30 and 9:40, with flow rates approximating 10 and 20 persons per minute, respectively. The arrival distributions of passenger flow at the intersection of the two routes and the starting point of the competition are

similar because of their proximity in distance. The arrival distributions rapidly increased and decreased over time, demonstrating higher peak flows. The peak flow at the intersection appears at approximately 9:55, with a rate of about 40 persons per minute. The passenger flow at the starting point of the competition peaks at around 9:57, reaching a rate of approximately 45 passengers per minute.

According to the video and questionnaire data, the average ticket-checking time was 6s per person. The average walking speed of spectators was  $u = 50m / min$ , and the variance was  $\sigma^2 = 20m^2 / min^2$ . 49% of the spectators choose to dwell at the Souvenir shop, with an average dwell time of 5.53 minutes and a variance of 2 min. 43% of the spectators choose to dwell at landscapes, with an average dwell time of 4.75 minutes and a variance of 1 min.

Based on the aforementioned survey results, the dynamic evolution model of inbound passenger flow was run using Matlab programs. Utilizing the passenger arrival data at the entrances as the initial input, the model is capable of predicting the passenger flow distributions at the intersection of the two routes and the starting point of the competition, as illustrated in Figures 4 and 5.

Overall, the predicted passenger arrival distribution aligns well with the survey data. However, there are some deviations observed during certain time periods, which can be partially attributed to the increased randomness in spectators' dwelling and walking behavior in cold weather conditions. To quantify the deviation between the predicted and actual passenger flow distributions, the Mean Absolute Percentage Error (MAPE) was employed. The prediction errors for the distribution at the intersection of the two routes and the starting point of the competition are 11.6% and 14.3%, respectively, both of which fall within an acceptable range. It suggests that the dynamic evolution model is well-suited for simulating the evolution of passenger flow across various nodes and can be effectively applied to different large-scale winter events.

For the application of the dynamic evolution model in upcoming large-scale events, only the arrival distributions of spectators at the first facility node during the entry process are required as input. Along with the provision of the total number of spectators, the start time of the event, information on facility nodes and the travel mode to be taken, the model can output the passenger distribution and queuing time distribution at each subsequent facility node.

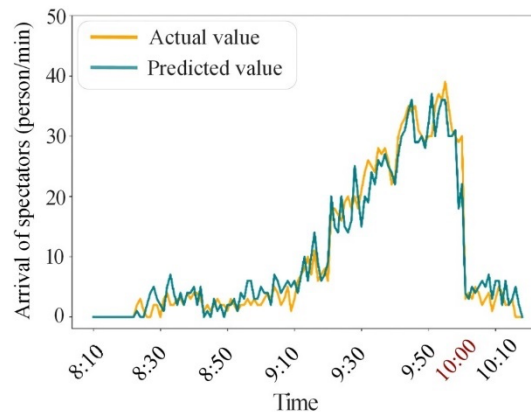


Figure 4. Passenger arrival distribution at the intersection of two routes

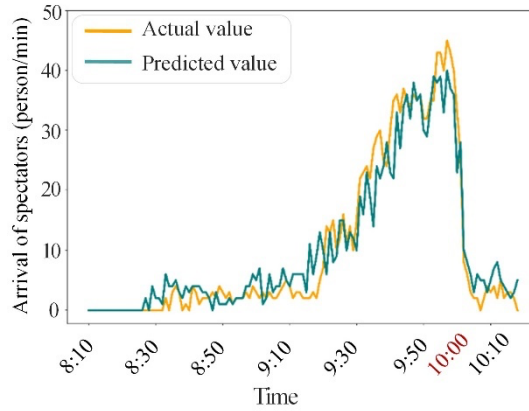


Figure 5. Passenger arrival distribution at the competition's starting point

## 4 Configuration optimization of service facilities based on node linkage and case analysis

### 4.1 Configuration optimization of service facilities based on node linkage

For large-scale events held in the outer suburbs, passenger flow moves dynamically and passes through different nodes on their journey from the urban transfer point to the venue. It is necessary to coordinate holistically in order to achieve a balanced passenger flow distribution and maintain the configured facilities at a reasonable service level. In this research, we have established a configuration optimization model of service facilities based on node linkage, which considers the passenger flow distribution at each node. This model integrates the benefits of spectators with the revenue of the event operator, enabling a collaborative optimization of the service facility configuration.

The configuration optimization model of service facilities, designed to minimize both the cost of spectator queuing time and the operational costs, is presented in Formula 19.

$$\min \gamma \times \alpha \times \sum_{t=0}^T \sum_{j=1}^J T_j(t) \times f_j(t) + (1 - \gamma) \times \sum_{j=1}^J \beta_j \times N_j \quad (19)$$

where  $\gamma$  is the objective weight, which ranges from zero to one.  $\alpha$  is the cost of queuing time and set as the local hourly wage in yuan per min.  $\beta_j$  is the unit cost of a service facility at node  $j$  in Yuan.

Considering the requirements for service level regarding to queue waiting time and the overall arrival rate of spectators for the event, the constraints of the model are shown in Formulas 20 and 21.

$$T_j(t) \leq T^{\max} \quad (20)$$

$$F_j(t_b) \geq 0.85 \times Q \quad (21)$$

Formula 20 shows that the mean queuing time of spectators at each node is less than the acceptable maximum time  $T^{\max}$  at a certain service level, which can be valued according to the survey data or relevant service standards. Formula 21 indicates that spectators who arrive at the venue before the start of the competition need to account for at least 85% of all spectators.  $t_b$  is the start time of a competition.  $Q$  represents the total number of spectators.

For the optimization model, the decision variable is  $N_j$ , which represents the number of service facilities configured at different nodes. The spectators' average queuing time, denoted as  $T_j(t)$ , is dependent on  $N_j$  and is estimated by the dynamic evolution model of passenger flow in Section 3. Therefore, the suitable facility configuration can be achieved through a combination of the dynamic evolution model and the optimization model. The models encompass a joint optimization of the number of facilities of each type and layout.

The Quantum Genetic Algorithm (QGA) is a probabilistic optimization algorithm formed by combining a Genetic Algorithm with quantum computing, and uses a unique quantum bit encoding mechanism. In comparison to the traditional Genetic Algorithm, the individuals encoded by quantum bits in the QGA always exist in a probabilistic form, thereby increasing the population diversity and the amount of information within the population (Lu, 2021). Meanwhile, the angle of the quantum rotation gate can be dynamically adjusted based on the fitness of individuals and enables them to evolve continuously in a more favorable direction. By adjusting the parameters of the quantum rotation gate, increasing the mutation probability, and introducing new individuals, QGA can avoid falling into local optimal solutions and promote the algorithm to continue searching for the global optimal solution. Consequently, the algorithm boasts advantages such as robust searching capabilities, reduced computing time, and rapid convergence speed, making it easy to converge towards a consistent optimal solution. It is particularly well-suited for nonlinear, complex, and multi-decision variable models. Additionally, the algorithm demonstrates remarkable robustness and flexibility when dealing with uncertain scenarios and models. Therefore, QGA is employed to solve the optimization model of service facilities configuration utilizing Matlab programming (Wang and Wei, 2021).

#### 4.2 Case analysis on optimization of service facilities configuration for large-scale events in outer suburbs

##### *A large-scale winter event in the outer suburbs and parameter settings*

In this research, a large-scale winter event to be held in the suburbs of Beijing was taken as illustrative case. The service facilities located along the route to the venue are currently being established. To encourage spectators to use a green, low-carbon travel mode, only public transport is available for spectators to travel from the urban transfer station to the venue. The initial layout of the service facilities comprises a remote security check and a proximal ticket check, as depicted in Figure 6.

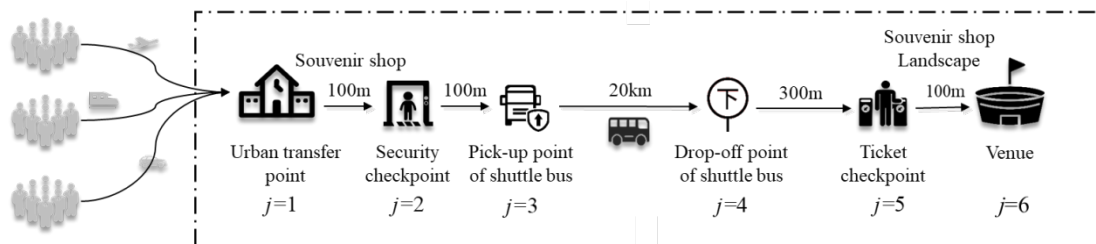


Figure 6. Distribution of main facility nodes along the entry process

The facility nodes that spectators need to pass through during their entry process include urban transfer points, security checkpoint, pick-up and drop-off points of shuttle buses, ticket checkpoint, and the venue, coded as  $j=1, 2, 3, 4, 5, 6$ . The distances between nodes and the distributed attractions are illustrated in Figure 6. The event commences at 10:00, and the total number of spectators is 3750. The first group of spectators who arrive at the urban transfer point is assumed at 7:00, with a duration of passenger arrival at this node spanning 150 minutes. The arrival distributions of spectators at different time intervals are detailed in Table 1.

**Table 1. Arrival distribution of spectators at the urban transfer point**

Time intervals	Before the start of competition					Total number of spectators
	3h-2.5h	2.5h-2h	2h-1.5h	1.5h-1h	1h-0.5h	
Arrival rate (%)	5	20	25	45	5	
Arrival of spectators	188	750	937	1687	188	3750

The security-checking time for spectators is 20 seconds per person. The mean ticket-checking time, walking speed of spectators, and dwell time at the souvenir shop and landscape are valued based on the survey data from Finlandia International Ski Marathon. The operating speed of the shuttle bus is 60 km/h. The capacity of shuttle bus is 50 persons. The purchase costs of the facilities are as follows: 2500 Yuan for a security check machine, 500 Yuan for a security gate, and 1000 Yuan for a ticket check machine. The rental cost of a bus is 1200 Yuan per day. The cost of the queuing time is 0.72 Yuan per minute.

Based on the questionnaire data, acceptable queue waiting times for security checks, ticket checks, and riding public transport were obtained and subsequently classified into different levels through cluster analysis, as presented in Table 2.

**Table 2. Classification of acceptable queue waiting time for different service facilities**

Service level for security or ticket check	Queue waiting time	Service level for riding shuttle bus	Queue waiting time
A (Very satisfied)	0~5min	A (Very satisfied)	0~4min
B (More Satisfied)	6~10min	B (More Satisfied)	5~9min
C (Generally satisfied)	11~16min	C (Generally satisfied)	10~15min
D (Dissatisfied)	17~24min	D (Dissatisfied)	16~23min
E (Very dissatisfied)	>24min	E (Very dissatisfied)	>23min

The proposed configuration optimization method for service facilities will be applied in the large-scale winter events. The maximum number of genetic iterations for the QGA used to solve the configuration optimization model is set at 100. The population size is 40 and the length of each binary variable is 20. The solution tends to be stable when it evolves to the 30th generation for each iteration, suggesting that the model demonstrates favorable convergence properties. Given the inherent randomness in spectators' initial arrival, as well as walking and dwelling behavior, both the evolution model of passenger flow and the optimization model of service facilities need to be run multiple times. The average values of the characteristic indices derived from these multiple runs are taken as the final output results.

#### *Configuration of facilities and passenger flow analysis under different objective weights*

For the configuration optimization model, three representative objective weight ratios were selected to analyze their influences on the number of configured service facilities and passenger flow distributions. The maximum queuing time in the optimization model is considered as the upper limit of the accepted range that corresponds to service level C, as outlined in Table 2. The capacity of service facilities at each node is not limited.

Under each assumed objective weight, both the evolution model of passenger flow and the optimization model were used to determine the optimal number of service facilities configured at each node, along with the associated total cost, as presented in Table 3. As can be observed, an increase in the objective weight assigned to spectators' queuing time cost leads to an increase in the number of configured service facilities at each node. This, in turn, results in a reduction in queuing time costs, improved service quality, and an increase in operational costs. Conversely, when the objective weight assigned to operational cost is increased, the number of configured service facilities at each node decreases, leading to a decrease in total operational costs but an increase in the total queuing time costs for spectators.

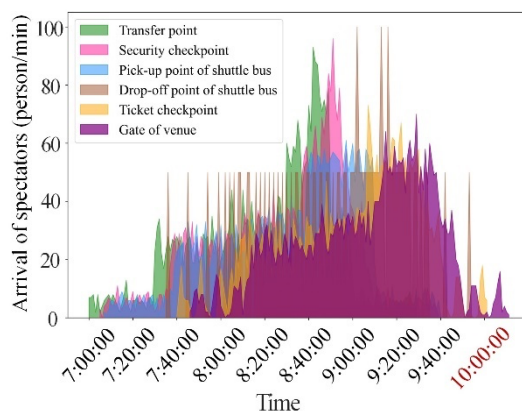
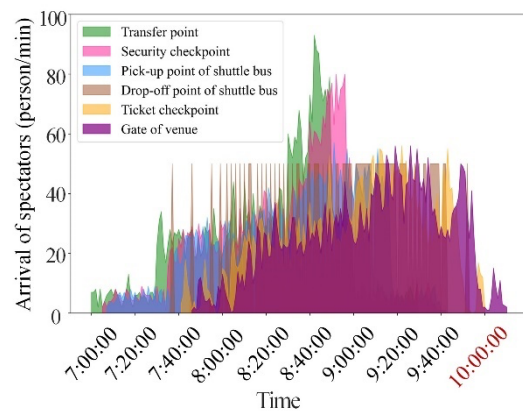
**Table 3. Optimal configured facilities and total cost under different objective weights**

Objective weight ratios	Number of security check machines	Number of shuttle buses	Number of ticket check machines	Total cost of queuing time of spectators (Yuan)	Total operation cost (Yuan)	Total cost (Yuan)
7:3	18	37	7	10607	105400	116007
1:1	15	32	6	15561	89400	104961
3:7	13	25	5	27200	74000	101200

Based on the configured service facilities detailed in Table 3, the statistics pertaining to passenger arrival, queuing time, number of spectators in queues, and relevant metrics are presented in Table 4. It can be seen that the greater the objective weight assigned to the queuing time cost, the higher the arrival rate of spectators before the start of the competition and the greater the maximum arrivals of spectators at the venue. It is evident that as the objective weight assigned to the cost of queuing time increases, so too does the arrival rate of spectators prior to the start of the competition, leading to a higher maximum number of arrivals at the venue. Furthermore, the mean queuing time for spectators at security checkpoints, pick-up points, and ticket checkpoints becomes shorter, accompanied by a decrease in the corresponding number of spectators in queues.

**Table 4. Passenger arrival and queue performance at nodes under different objective weights**

Objective weight ratios	7:3	1:1	3:7	
Arrival rate of spectators before the competition (%)	98.35	97.63	92.31	
Security checkpoint	Mean queuing time (minute per person)	0.29	1.02	1.77
	Maximum queuing time (minute)	6	10	16
	Maximum number of persons for queue	132	359	575
Pick-up point of shuttle bus	Mean queuing time (minute per person)	0.63	0.78	3.83
	Maximum queuing time (minute)	10	11	13
	Maximum number of persons for queue	94	95	92
Ticket checkpoint	Mean queuing time (minute per person)	0.09	0.17	0.34
	Maximum queuing time (minute)	1	1	1
	Maximum number of persons for queue	6	17	23
Venue	Maximum number of arrivals (person per minute)	71	53	40
	Mean number of arrivals (person per minute)	26	25	25

(a)  $\gamma (1-\gamma)=7:3$ (b)  $\gamma (1-\gamma)=1:1$



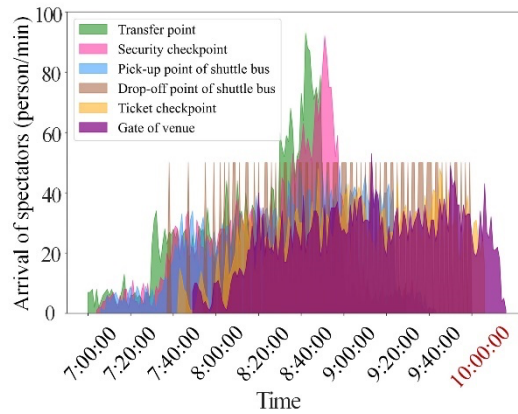
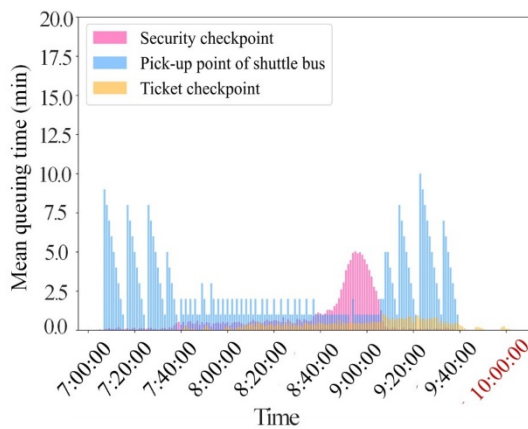
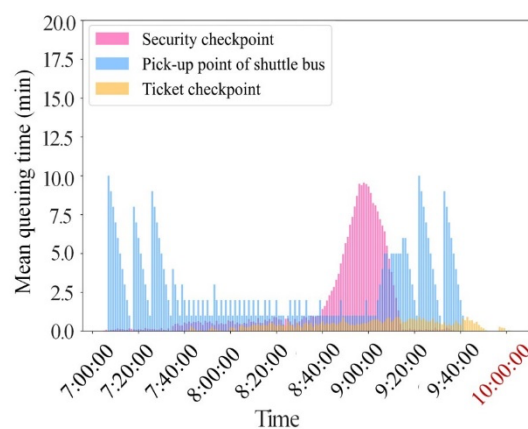
(c)  $\gamma (1-\gamma)=3:7$ 

Figure 7. Spectators' arrival distribution evolving among nodes under different objective weights

The dynamic evolution of passenger flow distribution is illustrated in Figure 7. Overall, the passenger flow undergoes a transition from a highly clustered state to a gently changing trend throughout the entry process. The arrival distribution of spectators at each node is primarily influenced by the passenger flow and service capacity of the facilities at its upstream nodes. Peak passenger flow is prone to occur at the upstream nodes. For instance, the passenger flow at the security checkpoint reaches a peak between 8:40 and 9:00, whereas the downstream nodes exhibit a relatively flat distribution.

When the weight ratio of spectators' queuing time cost and operation cost is 7:3, the passenger arrival distributions at all nodes show clustering passenger flow for a period of time, due to the presence of more configured service facilities, as depicted in Figure 7(a). Conversely, when the weight ratio for the dual-target costs shifts to 3:7, relatively fewer configured facilities lead to reduced service capacity at the upstream nodes, resulting in a higher clustering passenger flow in a short time period and decreased output flow at these nodes, as illustrated in Figure 7(c). As a result, passenger arrivals at their downstream nodes become more balanced and well-dispersed, with lower clustering, less peak flow, and reduced passenger pressure. When the weight ratio of the dual-target costs is equal at 1:1, Figure 7(b) reveals that the clustering phenomenon of passenger flow at the nodes can be mitigated to a certain extent. Additionally, the passenger flow at the downstream nodes is more evenly distributed, indicating that the service level of the facilities under this condition is relatively high.

(a)  $\gamma (1-\gamma)=7:3$ (b)  $\gamma (1-\gamma)=1:1$

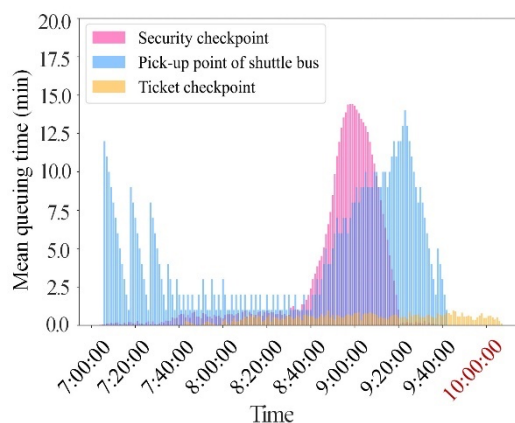
(c)  $\gamma(1-\gamma)=3:7$ 

Figure 8. Spectators' queuing time distribution among nodes under different objective weights

According to the passenger arrival distribution, the mean queuing time of spectators at the primary facility nodes can be determined. As depicted in Figure 8, the mean queuing time under different objective weights adheres to the preset acceptable threshold level of 16 min. Spectators at the security checkpoint experience a longer queuing time between 8:40 and 9:10 when the dual-target weight ratio is set to 7:3, as illustrated in Figure 8(a). Conversely, when the number of configured security check machines is reduced for the dual-target weight ratio of 3:7, Figure 8(c) reveals a significant increase in the queuing time of the passenger flow, with the extended queuing time interval spanning from 8:40 to 9:20.

Figures 8(a) and 8(b) demonstrate that there is a non-continuous clustering phenomenon of spectators during the initial and final stages of passenger arrival at the shuttle bus pick-up point. Passengers arriving during these two periods are fewer in number and are required to wait until the shuttle bus is fully occupied before being transported to the venue, leading to a longer waiting time. Figure 8(c) illustrates that long queues also form between 8:40 and 9:40 due to the less-configured shuttle buses. Overall, because the ticket checkpoint is located downstream of the entry process and has a relatively high service capacity of approximately 60 persons per minute, the mean queuing time of spectators remains low.

In general, when the weight on spectators' queuing time cost is greater, more configured service facilities and their accompanying high service capacity leads to shorter queuing times at all nodes and enhanced service levels, as demonstrated in Figure 8(a). Conversely, when the weight of operation costs is increased, Figure 8(c) reveals that a reduction in the number of configured service facilities significantly prolongs the queuing time for spectators at the security checkpoint and shuttle bus pick-up point, subsequently lowering the overall service level. The passenger flow distribution for a dual-target weight ratio of 1:1, as presented in Figure 8(b), lies between the extremes of these two conditions.

Taking into account both the queuing time cost and operation cost, as well as the passenger arrival distribution and queuing time, the reasonable dual-target weight ratio for the configuration optimization of service facilities is 1:1. Under this condition, the number of optimized configurations of facilities and operation costs are moderate, while ensuring a relatively even distribution of passenger flow and a suitable queuing time.

#### *Configuration of facilities and passenger flow analysis under different facility layout*

When it comes to service facilities for large-scale events held in the outer suburbs, security checks and ticket checks offer greater flexibility in their layouts because they can be located at the proximal and remote ends of the venue. Drawing upon the initial layout of remote security checks and proximal ticket checks from previous analysis, two distinct facility layout schemes were proposed:



one involving remote security and ticket checks, and the other featuring proximal security and ticket checks. These schemes are illustrated in Figure 9.

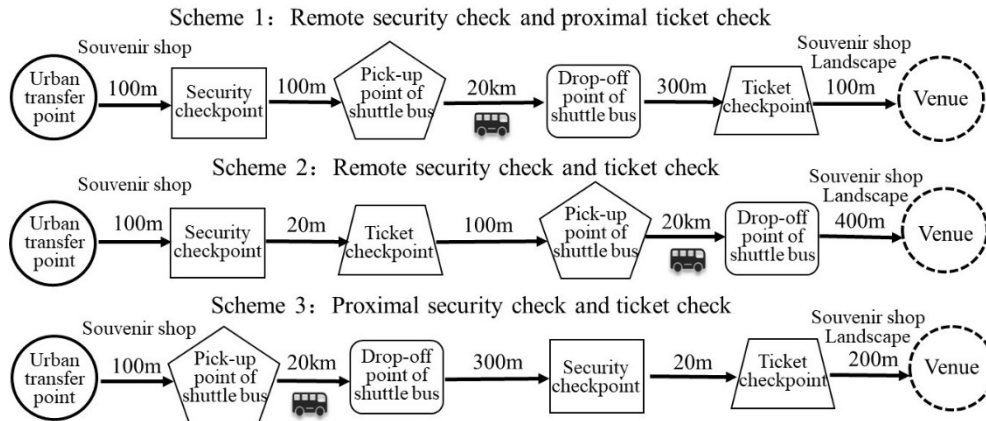


Figure 9. Layout schemes for security checking and ticket checking facilities

Based on the different layout schemes of service facilities, the dynamic evolution model and configuration optimization model are used to analyze the changes in the number of configured facilities, passenger arrivals, and queue performance under the unrestricted capacity of the facilities. For the optimization model, the objective weight ratio was set to 1:1, and the queuing time constraint was set as the spectators' maximum accepted value corresponding to service level C in Table 2.

As evident from Table 5, there are no significant differences in the optimal number of configured service facilities across the three layout schemes. Upon satisfying the spectators' accepted service level, the total cost of queuing time of spectators has little difference. Scheme 1, featuring remote security checks and proximal ticket checks, incurs the lowest total queuing time cost, closely followed by Scheme 2. Scheme 1 also has a minimum total cost.

Table 5. Optimal configured facilities and total cost under different facility layout schemes

Facility layout schemes	Number of security check machines	Number of shuttle buses	Number of ticket check machines	Total cost of queuing time of spectators (Yuan)	Total operation cost (Yuan)	Total cost (Yuan)
Scheme 1: Remote security check and proximal ticket check	15	32	6	15561	89400	104961
Scheme 2: Remote security and ticket check	15	32	7	16151	90400	106551
Scheme 3: Proximal security and ticket check	14	34	6	16359	88800	105159

Table 6. Passenger arrival and queue performance at nodes under different facility layout schemes

Facility layout schemes	Scheme 1	Scheme 2	Scheme 3
Arrival rate of spectators before the competition (%)	97.63	97.36	98.10
Security checkpoint	Mean queuing time (minute per person)	1.02	2.13
	Maximum queuing time (minute)	10	11
	Maximum number of persons for queue	359	370
Pick-up point of shuttle bus	Mean queuing time (minute per person)	0.78	1.10
	Maximum queuing time (minute)	11	12
	Maximum number of persons for queue	95	122

Ticket checkpoint	Mean queuing time (minute per person)	0.17	0.18	0.11
	Maximum queuing time (minute)	1	1	1
	Maximum number of persons for queue	17	33	6
Venue	Maximum number of arrivals (person per minute)	53	61	58
	Mean number of arrivals (person per minute)	25	25	25

The arrival distribution of passenger flow at each node under different facility layout schemes is depicted in Figure 10.

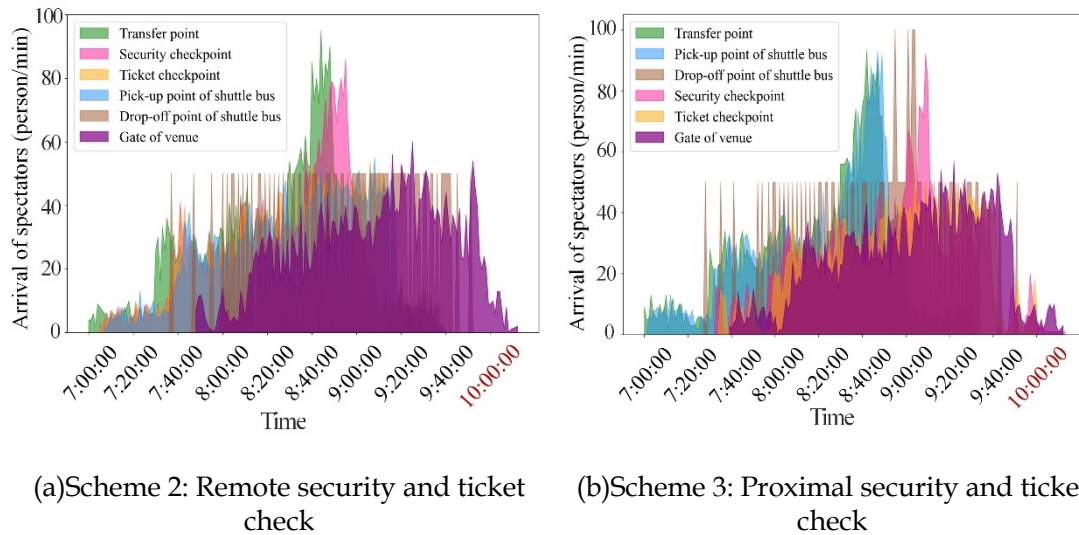


Figure 10. Spectators' arrival distribution evolving among nodes under different layout schemes

Compared with the distribution observed under Scheme 1, featuring remote security check and proximal ticket check in Figure 7(b), Table 6 and Figure 10(a) illustrate that implementing remote security check results in peak passenger flow formed at the upstream security checkpoint. This effectively alleviates passenger pressure and reduces queuing time at the downstream shuttle bus pick-up point. Additionally, it contributes to a more balanced arrival distribution at downstream nodes and mitigates the prominence of peak flows. The effectiveness for the layout scheme of remote security check and proximal ticket check is particularly evident.

As Figure 10(b) demonstrates, the layout of proximal security and ticket checks will lead to peak passenger flow at the shuttle bus pick-up point. However, this layout also reduces passenger pressure at the security and ticket checkpoints. Consequently, the average queuing time and maximum queue length at these two nodes experience significant decreases. Furthermore, Table 6 indicates that different facility layouts do not significantly influence the passenger arrival rate prior to the competition's start, the maximum passenger arrivals, or the average passenger arrivals at the venue.

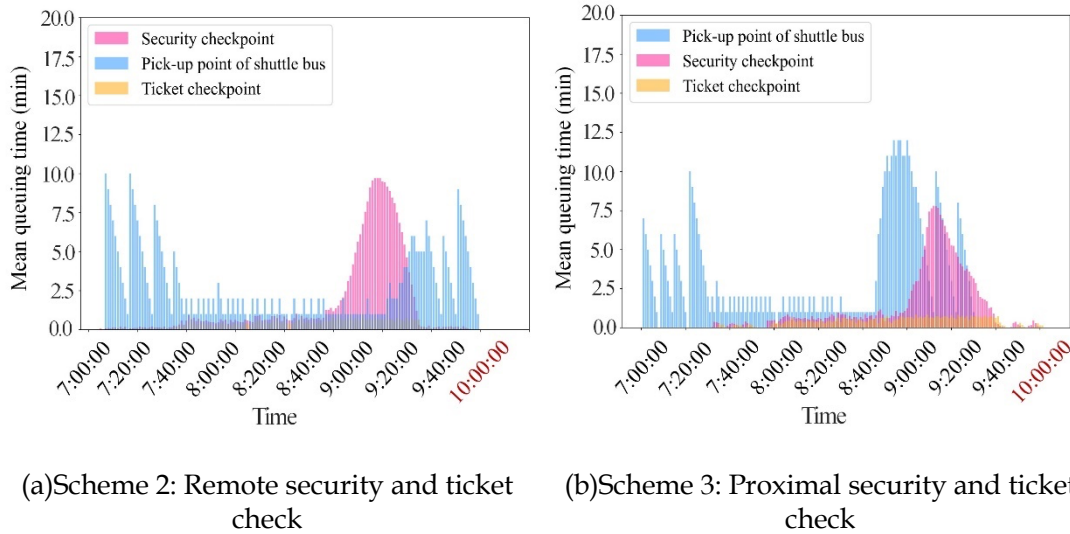


Figure 11. Spectators' queuing time distribution among nodes under different layout schemes

Compared with the spectators' queuing time distribution under Scheme 1, which involves remote security check and proximal ticket check in Figure 8(b), Figure 11 illustrates that the mean queuing time at the security checkpoint and of shuttle bus pick-up point undergoes significant changes with different layout schemes. However, the distributions at the ticket checkpoint exhibit little change. For the remote security check, as shown in Figure 8(b) and Figure 11(a), spectators' queues for security checks occur mainly between 8:40 and 9:10, with a longer mean queuing time of up to 9.8 minutes per person. Additionally, there is a noticeable queuing phenomenon at the shuttle bus pick-up point during the initial and final stages of passenger arrival. As for the proximal security and ticket check, Figure 11(b) demonstrates that the queuing passenger flow primarily occurs between 8:40 and 9:10 at the upstream pick-up point of the shuttle bus, whereas the queuing time at the downstream security node is significantly reduced.

Overall, there were no significant differences observed in the optimally configured service facilities across various layout schemes. A remote security check can effectively alleviate the passenger pressure at downstream nodes and reduce the total queuing time cost; however, it may lead to peak passenger flow at the security checkpoint. Specifically, Scheme 1, which incorporates remote security checks and proximal ticket checks, exhibits a more balanced distribution of passenger flow and provides a higher level of service quality. Proximal security and ticket checks can significantly reduce the queuing time, and the number of people queuing at these two nodes. For practical applications, selecting an appropriate facility layout based on the requirements of passenger flow organization and service level can enhance spectators' travel experience and satisfaction.

#### *Passenger flow organization with limited-service facilities*

Based on the large-scale winter event and parameter setting outlined in Section 4.2.1, the facility layout comprises a remote security check and proximal ticket check, and the weight ratio of the bi-objective function is 1:1, with the accepted maximum queuing time corresponding to the C-level. Under these conditions, Table 3 indicates that the optimal configuration of service facilities comprises 15 security check machines, 32 shuttle buses, and 6 ticket check machines. It is assumed that the space available for the security checkpoint is limited, allowing for the installation of only 10 security check machines. To assess the impact of this constraint, we employed the dynamic evolution model of passenger flow to analyze changes in the distributions of passenger arrival and queuing times as presented in Figure 12.

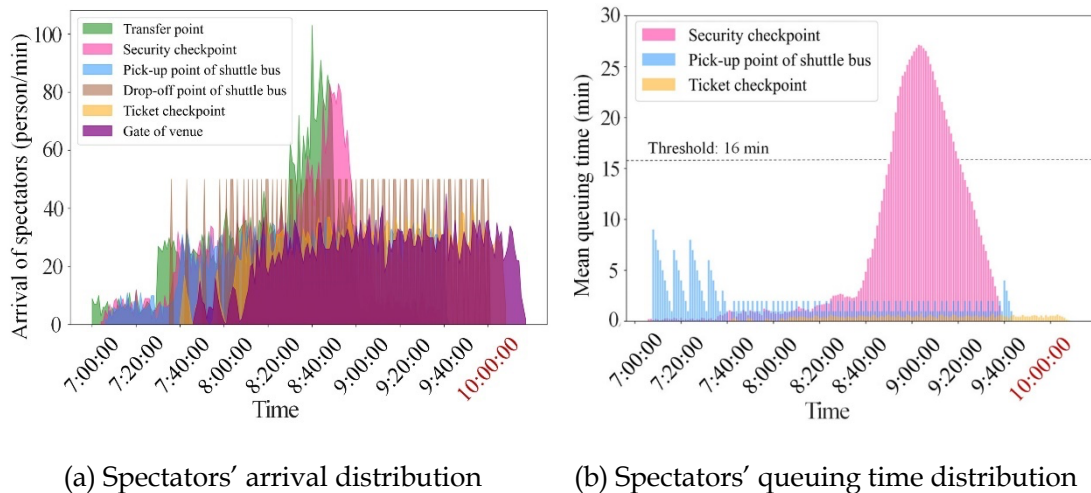


Figure 12. Passenger arrival and queuing time distribution under limited service facilities

Compared with Figure 7(b) and 8(b), Figure 12 demonstrates that the limited number of service facilities leads to higher clustering passenger flow and a significant increase in queuing time at the security checkpoint. Specifically, the queuing time between 8:50 and 9:20 exceeds the accepted maximum queuing time of 16 min, with the longest queuing time reaching 27 min. This situation significantly impacts spectators' travel experiences and necessitates optimization measures. On the other hand, the limited availability of security check facilities has a positive effect on the passenger flow distribution at the downstream locations, including the shuttle bus pick-up point, ticket checkpoint, and venue entrance. These areas experience a more balanced flow of passengers, with no notable peak flows.

- Improving measure 1: Adjustment of facility layout

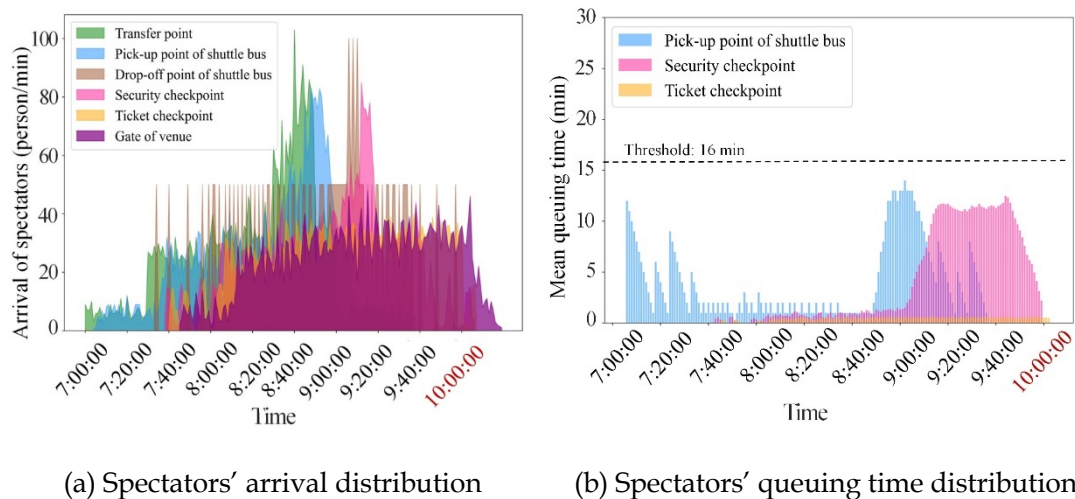


Figure 13. Passenger arrival and queuing time distribution for the adjusted facility layout

The original facility layout, which featured a remote security check, was adjusted to a proximal security check, while all other conditions remained constant. This change means that spectators need to take the shuttle bus to the drop-off point and proceed through the security check and ticket check sequentially to reach the venue. The resulting changes in passenger arrival and queuing time distributions are depicted in Figure 13.

As shown in Figure 13, shifting the security checkpoint to the downstream of the entry process results in a peak passenger flow at the upstream pick-up and drop-off points of the shuttle bus. However, the limited number of machines at the security checkpoint contributes to a more balanced distribution of passenger arrivals at the downstream ticket checkpoint and venue

entrances. Consequently, the period during which spectators continuously queue at the security checkpoint shifts downstream, and the corresponding average queuing time is significantly reduced. The maximum average queuing time is 12.6 minutes, which meets the spectators' accepted threshold

- Improving measure 2: Passenger flow control at upstream nodes

In cases where adjusting the facility layout is not feasible, passenger flow control at upstream nodes of the security checkpoint can serve as an effective alternative strategy. Measures such as providing clear guidance information, adding attractions, and reducing the service capability of certain facilities can be used to reduce passenger arrival at the urban transfer point. It is assumed that the decrease in the controlled passenger flow was maintained at 10% each time. Then, the dynamic evolution model of passenger flow is used to obtain the spectators' average queuing time at each node, which is further evaluated with spectators' accepted maximum queuing time corresponding to the C-level. It was found that when the passenger flow during the peak period, which occurs 1.5 to 1 hour before the start of the competition is reduced by 20% at the urban transfer point and shifted backward to an off-peak period, the average queuing time is significantly reduced. Specifically, the maximum average queuing time drops to 15 minutes, which falls within the spectators' accepted threshold for the desired service level.

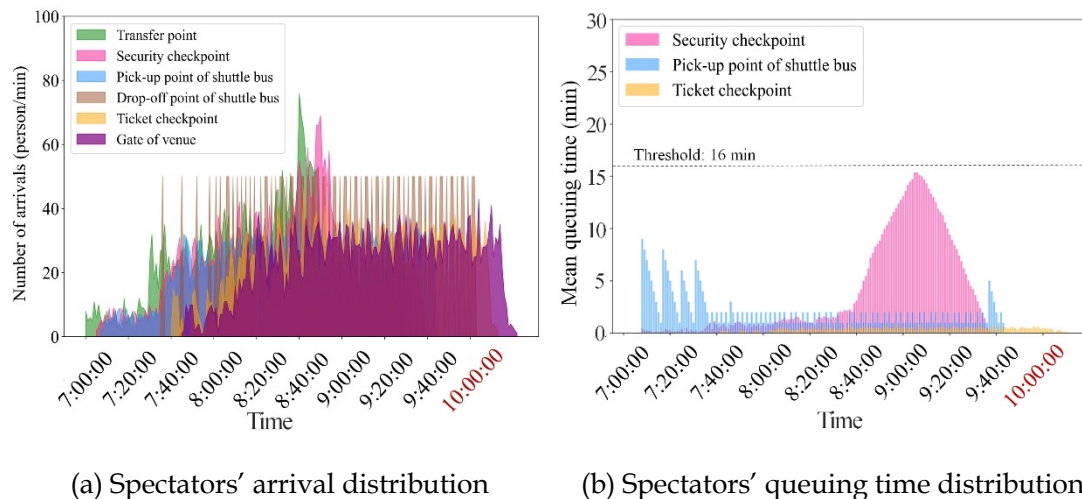


Figure 14. Passenger arrival and queuing time distribution for the flow control of upstream nodes

Figure 14 demonstrates that implementing passenger flow control for upstream nodes can make the passenger arrival distribution among nodes relatively flat. This approach eliminates noticeable peak flows and alleviates passenger pressure at downstream nodes.

## 5 Conclusions

As the economy rapidly progresses, there has been a surge in the number of large-scale winter events being hosted across various regions. A well-planned and reasonable configuration of service facilities is vital for ensuring the smooth and successful execution of large-scale events. This study focuses on large-scale events held in the outer suburbs of cities. A dynamic evolution model of passenger flow was developed and validated using actual survey data. This model can better simulate passenger arrival distribution evolving among nodes and predict the mean queuing time and queue sizes over time during the spectators' entry process. Furthermore, we introduce an optimization approach for service facility configuration, leveraging node connectivity. Applying this framework to a large-scale winter event, the following conclusions were derived:

Regarding the optimization method, assigning a higher objective weight to the spectators' queuing time cost can lead to an increase in the number of configured service facilities and corresponding operation costs, thereby effectively enhancing service quality. When equal weights are given to



both the spectators' queuing time cost and the operation cost, the number of configured facilities and the operation cost tend to be moderate. A well-balanced passenger flow distribution and suitable queuing times can be achieved.

Under different layout schemes of service facilities, there are no significant differences in the optimal number of configured service facilities and spectator queuing time costs. A remote security check can alleviate the passenger pressure at downstream nodes and reduce the total queuing time cost, especially when combined with proximal ticket checks. However, peak passenger flows may still occur at security checkpoints. Implementing proximal security and ticket checks can reduce the queuing time, and the number of people in the queue at these two nodes. A suitable facility layout could be chosen according to the requirements of passenger flow organization and service level, thus promoting spectators' travel experience and satisfaction.

The limited-service facilities provision can lead to increased passenger clustering, significantly longer queuing times for spectators, and a detrimental impact on their travel experience. To address this, the dynamic evolution model of passenger flow and the configuration model of service facilities can be utilized to coordinately optimize passenger flow at nodes through measures such as adjusting the facility layout, controlling passenger flow, and diverting traffic. By doing so, a good match between passenger flow distribution and facility service capacity can be achieved to make the passenger arrival among nodes relatively balanced and reduce peak flow and passenger pressure.

These findings can serve as a valuable reference for the analysis of passenger flow, service facility configuration, and passenger flow organization for large-scale events in the outer suburbs. In the future, it will be necessary to further enrich the passenger flow data for large-scale events and fully validate the dynamic evolution model of passenger flow, as well as the optimization model for facility configuration. Additionally, an in-depth exploration of spectators' dwell behavior can enhance our ability to accurately predict passenger flow distribution at large-scale events.

## Funding

This study was financially supported by the following fundings: Beijing Natural Science Foundation of China (8212002), National Natural Science Foundation of China (71971005) and National Scholarship Foundation of China (202106545001).

## Data availability

The data that support the findings of this study are available from the corresponding author upon request.

## Contributor Statement

Conceptualisation: Huanmei Qin, Meiru Jia.

Data Collection and Analysis: Meiru Jia, Yonghuan Zhang, Cui Qian.

Funding Acquisition: Huanmei Qin.

Methodology: Meiru Jia.

Algorithm: Meiru Jia.

Writing - Original Draft: Huanmei Qin, Meiru Jia.

Writing -Revision & Editing: Huanmei Qin, Meiru Jia, Yonghuan Zhang, Cui Qian.

## Acknowledgements

The authors thank the anonymous reviewers for their valuable comments and suggestions. This research was supported by the Beijing Natural Science Foundation (8212002; L201008), National Natural Science Foundation (71971005) and National Scholarship Foundation of China (202106545001).

## Conflict Of Interest

There is no conflict of interest.

## References

- Ding Y, Lv Z Q, Chen T, et al. Study on Optimization Model of Airport Passenger Security Check Queuing Management. 2018 11th International Symposium on Computational Intelligence and Design (ISCID). IEEE, 2018, 2: 281-286.
- Fellendorf M. Traffic Modelling of Large Events—A Summary of Selected German Examples. IFAC Proceedings Volumes. 2006, 39(12): 17-24.
- Frantzeskakis J M. Athens 2004 Olympic Games: transportation planning, simulation and traffic management. *Ite Journal*, 2006, 76(10): 26-32.
- Karlaftis M G, Kepaptsoglou K, Stathopoulos A. Decision support systems for planning bus operations during mega events: The Athens 2004 summer olympics. IFAC Proceedings Volumes, 2006, 39(12): 210-215.
- Liu J M, Qi X Q, Xu Y M, et al. Queuing Strategy Optimization with Restricted Service Resources. *Wireless Personal Communications*, 2018, 102(4): 2681-2699.
- Li W, Zhou M, Dong H R. Forecasting Model and Control Strategy of Large Passenger Flow under Large-scale Activity Conditions. 2019 3rd Advanced Information Management, Communicates, Electronic and Automation Control Conference (IMCEC). IEEE, 2019: 438-442.
- Liu R M, Li S K, Yang L X. Collaborative optimization for metro train scheduling and train connections combined with passenger flow control strategy. *Omega*, 2020, 90: 101990.
- Lu T C. CNN Convolutional layer optimisation based on quantum evolutionary algorithm. *Connection Science*, 2021, 33(3): 482-494.
- Matthew G K, Kepaptsoglou K, Stathopoulos A. A Decision Support System for Special Events Public Transport Network Planning: The Case of the Athens 2004 Summer Olympics. TRB Annual Meeting [CD]. 2004.
- Roper D H. Los Angeles, 1984 Olympic games. *Transportation Research Board Special Report*, 1987, 55(3): 26-27.
- Wang X R, Wu J J, Yang X, et al. Multistation coordinated and dynamic passenger inflow control for a metro line. *IET Intelligent Transport Systems*, 2020, 14(9): 1068-1078.
- Wang Y, Wei C Y. Design optimization of office building envelope based on quantum genetic algorithm for energy conservation. *Journal of Building Engineering*, 2021, 35: 102048.
- Wang H Y, Li L Y, Pan P J, et al. Early warning of burst passenger flow in public transportation system. *Transportation Research Part C: Emerging Technologies*. 2019,105: 580-598
- Wang X, Li S K, Tang T, et al. Event-Triggered Predictive Control for Automatic Train Regulation and Passenger Flow in Metro Rail Systems. *IEEE Transactions on Intelligent Transportation Systems*. 2022, 23(3): 1782-1795.
- Wei Z H, Wu Y Y, Li Y. Application of pedestrian simulation software in Beijing Olympic Games: a case study of Olympic badminton venue. 2009 WRI World Congress on Software Engineering. IEEE, 2009, 2: 254-261.
- Yi J. The Research of Passenger Flow Through Checkpoint Based on Queuing Theory. 2nd International Conference on Machinery, Electronics and Control Simulation (MECS 2017). Atlantis Press, 2016.
- Yin Y, Li D, Zhao K, et al. Optimum equilibrium passenger flow control strategies with delay penalty functions under oversaturated condition on urban rail transit. *Journal of Advanced Transportation*, 2021.
- Yoo S, Kim H, Kim W, et al. Controlling passenger flow to mitigate the effects of platform overcrowding on train dwell time. *Journal of Intelligent Transportation Systems*, 2022, 26(3): 366-381.

Zhang Y C. Modeling traffic impact under special events. The University of Akron, 2003.

Zhang Z, Weng J C, Wang L X, et al. Study on the influencing factors and passenger volume analysis of lasting large scale activities. 2015 International Conference on Transportation Information and Safety (ICTIS). IEEE, 2015: 414-418.